Article citation info:
Żardecki D, Dębowski A. Method of analysing torsional vibrations in the motorcycle steering system in the phase plane. The Archives of Automotive Engineering – Archiwum Motoryzacji. 2017; 76(2): 137-154, http://dx.doi.org/10/14669/AM.VOL.76.ART8

METHOD OF ANALYSING TORSIONAL VIBRATIONS IN THE MOTORCYCLE STEERING SYSTEM IN THE PHASE PLANE

DARIUSZ ŻARDECKI[1], ANDRZEJ DĘBOWSKI[2]
Military University of Technology (WAT)

Summary

A vibration analysis method has been described, where time functions are represented in the "phase plane"; for free vibrations, the representations are classic phase portraits. In the case of vibrations forced with sinusoidal inputs, the representations are Lissajous figures and their stroboscopic expansions to "Poincaré maps". For the purposes of presentation of the research method proposed, the analyses of free and forced vibrations of a system close to the motorcycle steering system have been described, with the system being modelled and simulated in the Matlab-Simulink environment and with the stick-slip processes being taken into account. The calculation results depict not only the essence of the method of analysing vibrations in the phase plane but also the impact of selected model parameters (in this case, related to freeplay and friction) and measurement disturbances on the representation results. The analysis method shown is a solution alternative to the classic spectral analyses.

Keywords: torsional vibrations in the motorcycle steering system, vibration modelling and simulation, freeplay and friction effects, stick-slip, vibration analysis in the phase plane, model sensitivity analysis

1. Introduction

The torsional vibrations occurring in the steering system and steered wheel constitute an important problem for motorcycle users due to their impact on driving safety and comfort. This is evidenced by descriptions of vibrations of this kind observed in single-track vehicles moving with high speeds; such vibrations often cause instability of vehicle motion and, in consequence, accidents. Thus, the torsional vibrations in the motorcycle steering system still constitute an open engineering problem and, for theoreticians and researchers

[1] Military University of Technology (WAT), Faculty of Mechanical Engineering, ul. Gen. S. Kaliskiego 2, 00-908 Warszawa, Poland; e-mail: dariusz.zardecki@wat.edu.pl

[2] Military University of Technology (WAT), Faculty of Mechanical Engineering, ul. Gen. S. Kaliskiego 2, 00-908 Warszawa, Poland; e-mail: andrzej.debowski@wat.edu.pl

engaged in the dynamics of vehicle motion, they are an important and interesting scientific challenge [6, 12].

The torsional vibrations in vehicle steering systems may result from various reasons. They may be forced directly, e.g. by wheel unbalance, or indirectly, e.g. by road surface irregularities; in the latter case, they very strongly depend on vehicle speed, as the excitation frequency directly depends on the rotational velocity of vehicle wheel. The unforced (free) vibrations have their source in the dynamic structure of the steering system. Due to spring elements present in the system, this structure may happen to become, in certain conditions, a vibration generator even at small momentary excitation (the shimmy effect). In many cases, the reasons for, and the effects of, the vibrations may be quite complex. On the one hand, the vibrations may be forced by various factors; on the other hand, free vibration processes may be encountered. In some specific circumstances, i.e. when the excitation frequency is identical with the natural system frequency (at a resonance), the system response to the excitation may be very strong.

Due to its mechanical structure, the motorcycle steering system is a dynamic one. Therefore, its torsional vibrations must be analysed in compliance with the general rules of the analysis of vibrations in dynamic systems. The vibrations in a dynamic system may be linear or non-linear, depending on the linear or non-linear nature of the mathematical model of the system.

When the dynamic model is linear, then, following the cessation of the transient process, the system response to a sinusoidal input is also sinusoidal, with an identical frequency at that, except that it is phase-shifted. The amplification factor and phase shift between the signals are directly determined by the system transmittance and they do not depend on the excitation amplitude; conversely, they depend on the frequency [7]. Hence, the key factors in the analysis of vibrations of a linear system are the frequency response characteristics of the magnitude and phase angle, based on the system transmittance and independent of the input. Since the profile of any input may be defined by the superposition of its harmonic components, the frequency response characteristics constitute, in linear systems, the basic tool for the analysis of vibrations forced by any inputs. The vibrations in linear systems are also analysed, although less frequently, with the use of methods based on time functions visualized in the phase plane with the elimination of time. In the case of forced vibrations, especially when a sinusoidal excitation is applied to the system input, curves referred to as "Lissajous figures" are plotted. The analysis of vibrations in linear systems has already become a sort of "classics", present in numerous works carried out in various fields of exact sciences and technology.

When the dynamic system is non-linear and a sinusoidal input is applied to it, the magnitude and phase responses depend not only on the frequency but also on the amplitude of the input [3]. If the input is freely shaped, the rule of superposition of the harmonic components in the response curve does not hold. Therefore, the role of frequency response curves in such a case is far less important. For a non-linear system, the vibration analysis must be based on the analysis of time functions. This is the case in particular when vibrations in a mechanical system are analysed with taking into account the stick-slip processes accompanying the dry friction effect or when the non-linearity of vibrations arises from

the presence of freeplay in spring joints [17]. Such a situation is also encountered when deterministic chaos breaks out in a non-linear system due to its singular structure, i.e. when the system response to a sinusoidal input with a specific amplitude and frequency is a random process with a wide spectrum [9]. This brings about interesting scientific challenges, i.e. questions how to utilize and process the time functions so that conclusions about the non-linear vibrations observed in the system could be formulated on these grounds, or how to ascertain the occurrence of stick-slip processes, freeplay-related disappearance of vibrations, or breaking out of deterministic chaos. A number of interesting proposals of research tools to analyse non-linear vibrations in the phase plane can be found in the literature dealing with this subject, e.g. visualizations in the form of Lissajous figures and their stroboscopic expansions to "Poincaré maps" [4].

This article shows possible applications of the representations in the phase plane for the analysis of vibrations in a motorcycle steering system, especially non-linear vibrations in the presence of freeplay and friction. The methods proposed have been presented with the use of computer simulation. Thanks to this, not only the impact of changes in parameters of the non-linear model but also the influence of measurement disturbances on changes in the representation forms may be investigated, which is a matter of considerable importance in the research practice.

2. Theoretical foundations of the vibration analysis in the phase plane

We are considering a model of a dynamic system (linear or non-linear) expressed by vector equations of state (1) and outputs (2):

$$\dot{\underline{x}}(t) = \underline{f}(\underline{x}(t), \underline{w}(t)) \tag{1}$$

$$\underline{y}(t) = \underline{h}(\underline{x}(t), \underline{w}(t)) \tag{2}$$

When the system is autonomous, i.e. no inputs $\underline{w}(t)$ are applied to it, then the response functions $y(t)$ resulting from non-zero initial conditions $x(t_0)$ are functions whose equivalents in the vibration theory are free vibrations.

When the system is non-autonomous, but it is in the conditions of dynamic equilibrium at the initial instant, i.e. when $\underline{f}(\underline{x}\ (t_0), \underline{w}(t_0))=0$, then the response functions resulting from the application of non-zero inputs w(t) are functions whose equivalents in the vibration theory are forced vibrations.

The scalar representation yi(yk) is a "phase portrait" of the pair of variables yj(t) and yk(t) with time t having been eliminated. For dynamic systems with multiple inputs and outputs, multiple phase portraits may be talked about. In the case of a system with a single input and a single output, a single-phase portrait is dealt with.

When the output variables y(t) have been appropriately defined, the phase portraits may represent e.g. functions of the following type:

– $\dot{x}_k(x_k)$, used in the analyses of processes in autonomous systems;
– $x_j(w_k)$, used in the analyses of processes in non-autonomous systems.

The phase portraits are also sometimes used for determining equivalent non-linear characteristic curves. As an example: in dry-friction systems, which are based on Coulomb characteristics of the $F_C(\dot{x})$ type, they are used for determining characteristic curves with hysteresis $F_h(x)$ [11].

The Lissajous figures are the phase portraits applicable to the cases where the independent variable in representation $y_j(y_k)$ has the form of a periodically varying quantity. Most frequently, such representations are used in the analysis of non-autonomous systems with a single input $w(t)$ and a single output $y(t)$, responding to a sinusoidal excitation $Asin(\omega t)$. Their geometrical forms $y(w)$ depend on the properties of the specific dynamic system. The determining of the Lissajous figures is an element of the computing and measuring systems used, e.g. LabVIEW [14].

In the case of stationary linear systems, an analytical formula $u(w)$ with time having been eliminated may be obtained through the use of simple mathematical "tricks". Namely, according to the properties of stationary linear systems:

$$\text{if } w(t) = Asin(\omega t) \qquad \text{then } y(t) = B(\omega)(sin(\omega t + \varphi(\omega)) \tag{3), (4}$$

Hence, in turn, we obtain:

$$sin(\omega t) = \frac{w(t)}{A}; \tag{5}$$

$$sin(\omega t + \varphi(\omega)) = sin(\omega t)\,cos(\varphi(\omega)) + cos(\omega t)\,sin(\varphi(\omega)) = \frac{y(t)}{B(\omega)}; \tag{6}$$

$$\frac{w}{A}cos(\varphi(\omega)) + \sqrt{1-\left(\frac{w}{A}\right)^2}\,sin(\varphi(\omega)) = \frac{y}{B(\omega)}; \tag{7}$$

$$\left(1-\left(\frac{w}{A}\right)^2\right)sin^2(\varphi(\omega)) = \left(\frac{y}{B(\omega)} - \frac{w}{A}cos(\varphi(\omega))\right)^2 \text{; and} \tag{8}$$

$$sin^2(\varphi(\omega)) - \left(\frac{w}{A}\right)^2 sin^2(\varphi(\omega)) = \left(\frac{y}{B(\omega)}\right)^2 - \frac{2y_j y_k\,cos(\varphi(\omega))}{B(\omega)A} + \left(\frac{w}{A}\right)^2 cos^2(\varphi(\omega)) \tag{9}$$

– At a zero phase shift (for a static system, $\varphi(\omega) = 0$, $B(\omega) = \mathrm{B}$), the following, in succession, may be obtained from (9):

$$\left(\frac{y}{B}\right)^2 - \frac{2yw}{BA} + \left(\frac{w}{A}\right)^2 = 0; \qquad \left(\frac{y}{B} - \frac{w}{A}\right)^2 = 0 \text{; and} \qquad y = \frac{B}{A}w \tag{10), (11), (12}$$

The resulting formula (12) is, in the (w, y) coordinate system, an equation of a straight line.

– At a non-zero phase shift $(\varphi(\omega) > 0)$, formula (9) may be transformed into equation (13), which represents, in the (w, y) coordinate system, an ellipse with the centre at a point (0, 0), inclined at an angle of $\varphi(\omega)$. The ellipse aspect ratio depends on the amplitudes and phase shift; therefore, its values vary with ω.

$$\left(\frac{y}{B(\omega)\sin(\varphi(\omega))}\right)^2 - \frac{2yw\cos(\varphi(\omega))}{B(\omega)A\sin^2(\varphi(\omega))} + \left(\frac{w}{A\sin(\varphi(\omega))}\right)^2 = 1 \tag{13}$$

Let us note that if $\varphi(\omega) = \pi/2$ and $B(\omega) = A$ then equation (13) represents a circle.

A typical Lissajous figure for a stationary linear system has been shown in Fig. 1.

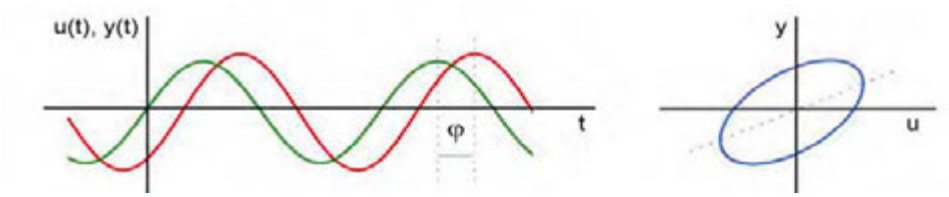

Fig. 1. Example of a Lissajous figure for a linear stationary dynamic system

In the case of non-stationary linear systems (which include parameters slowly changing with time), the corresponding Lissajous figures are closed curves evolving with time.

In the case of non-linear systems, no general analytical formula $y(w)$ with time having been eliminated can be obtained. As is widely known, the response of such systems to a sinusoidal input is a polyharmonic time function (which includes sinusoidal components with frequencies different from the input frequency) or even a chaotic signal. The Lissajous figures may then have "strange" irregular forms of even forms varying with time, significantly differing from the simple ellipses occurring for stationary linear systems. To confirm this fact, several examples of simple representations $y(w)$ obtained for $w(t) = \sin(\omega t)$ and $y(t) = \sin(k\omega t+\varphi)$ [10] have been presented in Fig. 2.

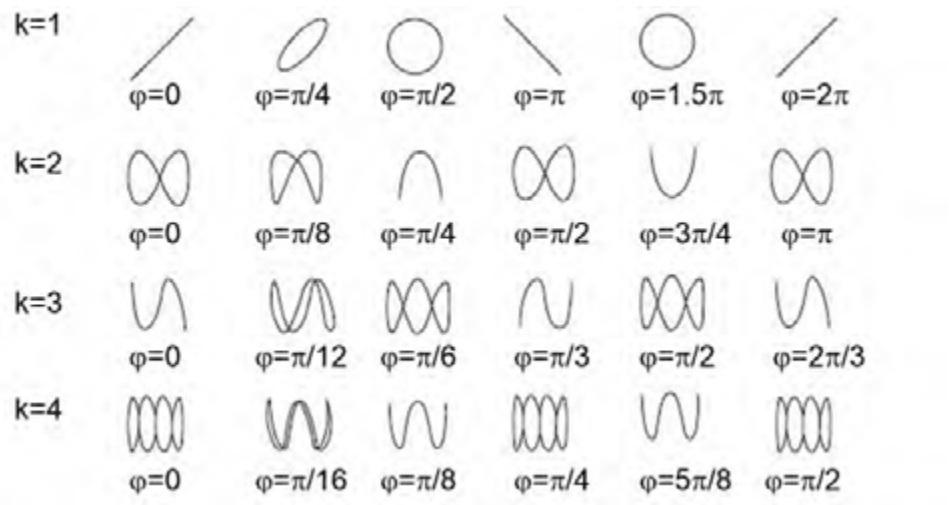

Fig. 2. Lissajous figures for time functions $w(t) = sin(\omega t)$ and $y(t) = sin(k\omega t+\varphi)$

The figures most similar to those obtained for stationary linear systems are the curves plotted for quasi-linear and quasi-static systems, when the input is slowly changing with time and no significant phase shift takes place (Fig. 3).

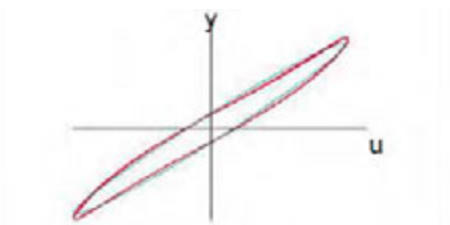

Fig. 3. Example of a Lissajous figure having the form of a deformed ellipse

The most irregular Lissajous figures are obtained when the system response to a sinusoidal input is a chaotic signal.

To detect singularities, especially chaos, in the functioning of non-linear dynamic systems, a solution referred to as "Poincaré maps" is used. Such maps are visual displays $y(u)$ generated by sampling the signals under analysis with a frequency of the sinusoidal signal applied at the system input (which results in a stroboscopic effect). Thanks to this, a dot image showing the nature of the response is generated in plane (u, y). When a Poincaré

map consists of one point, this indicates that the response is also a sinusoid of the same frequency; when the map consists of two points, the response has two components, and so on. In a chaotic process, a cloud of points is obtained and the shape of such a cloud may be a valuable source of information about the process under analysis. An example of such a display has been shown in Fig. 4.

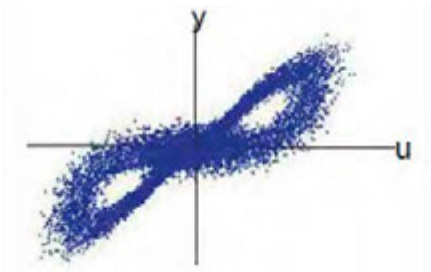

Fig. 4. Example of a Poincaré map for a system with chaotic dynamics

The Lissajous figures and their expansions to Poincaré maps may constitute effective tools for the analysis of vibrations in a system under examination; they may also be used for the identification of a model of the system. Obviously, deep exploration with the use of extensive simulation tests is required for every model structure.

3. Mathematical model of torsional vibrations in the motorcycle steering system

To examine the applicability of the Lissajous figures and Poincaré maps for the analysis of torsional vibrations in the motorcycle steering system, the model previously used in the work described in [18] was adopted. Such a single-body model reflects the most important attributes of the steering system dynamics and simultaneously makes it possible to analyse torsional vibrations in the presence of "sharp" non-linearities arising from the free-play and friction effects. However, the aspect of tyre-road interaction is disregarded in it because, if otherwise, the model would be much more complicated without any impact in this case on the analysis method. A concept of the modelling has been illustrated in Fig. 1.

Fig. 5. A concept of the equivalent model used for testing the numerical procedures

The test model adopted corresponds to a situation where the handlebar is fixed. The torsional vibration of the wheel may be caused by the application of a variable external moment of forces (e.g. due to wheel unbalance) or by twisting the system to move the wheel out of its angular position of equilibrium and then releasing it free. This equivalent steering system model adopted is actually a torsional pendulum where a twisted rigid inert element (the wheel) is coupled with a weightless elastic shaft (linear elasticity) mounted with a freeplay in a housing. The shaft of the inert element is placed in a housing bearing. The bearing acts on the twisting motion through viscous friction forces (linear damping) and dry friction forces (dry kinetic and static friction, which causes the stick-slip phenomenon).

The mathematical model that describes the torsional vibrations of the wheel (nonlinear because of the impact of freeplay and friction) may have the form of a second-order differential equation with variable structure [17, 18]:

$$J\ddot{\alpha}(t)=\begin{cases} M_w(t)-k\cdot luz(\alpha(t),\alpha_0)-\mu\cdot tar\left(\dot{\alpha}(t),\dfrac{M_{TK0}}{\mu}\right), & if\ \dot{\alpha}(t)\neq 0 \\ luz\left(M_w(t)-k\cdot luz(\alpha(t),\alpha_0),M_{TS0}\right), & if\ \dot{\alpha}(t)=0 \end{cases} \tag{14}$$

The conditions $\dot{\alpha}(t)\neq 0\ /\ \dot{\alpha}(t)=0$ have been taken from the Coulomb friction model [1]. In numerical calculations, the controlling of variability of the structure by adopting the conditions $|\dot{\alpha}(t)|>\varepsilon$ and $|\dot{\alpha}(t)|\leq\varepsilon$, where ε is a parameter of a "small" value, is also allowed, as it is in the Karnopp model [1].

Notation:

J – moment of inertia; μ – damping coefficient (for viscous friction); M_{TK0} – moment of dry kinetic friction forces; M_{TS0} – maximum value of the moment of dry static friction forces; k – stiffness coefficient; α_0 – angular freeplay parameter; α – angle of torsion; M_w – moment of the external input force; t – time.

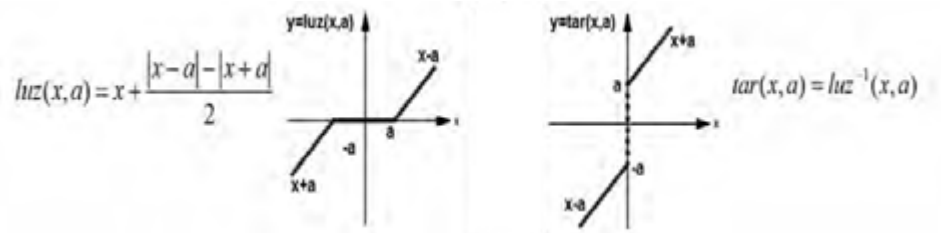

Fig. 6. Geometrical interpretation of the luz(...) and tar(...) representations

The *luz*(...) / *tar*(...) representations make it possible to express analytically the characteristic curves of stiffness (a curve with a "dead" zone caused by the freeplay) and kinetic friction force (a Coulomb curve, which is a superposition of a linear function and a pseudo-function *signum*(...)) and, moreover, to express the stick-slip process in the neighbourhood of zero velocity [15, 16, 17].

The torsional vibrations of the pendulum may be simulated with excitation exclusively coming from non-zero initial conditions (it would be then $M_w(t) = 0$) or with preset external excitation $M_w(t)$ (with zero initial conditions in this case). The excitation coming from non-zero initial conditions leads to a situation where dry static friction develops and the motion is blocked (with the velocity being constant and equal to zero and the angular position remaining unchanged). The external excitation $M_w(t) = M_{w0}sin(\omega t)$ will make it possible to examine the applicability of the Lissajous figures and Poincaré maps for the vibration analysis per se as well as for the identification of unknown model parameters based on actual vibration records. For the simulated curves to be as close as possible to the curves actually obtained from measurements carried out on a real object, curves disturbed by noise will also be examined.

Let us note that in the absence of freeplay ($\alpha_0 = 0$) and dry friction ($M_{TK0} = M_{TS0} = 0$), the non-linear equation (14) becomes a linear one:

$$J\ddot{\alpha}(t) + \mu\dot{\alpha}(t) + k\alpha(t) = M_w(t) \tag{15}$$

When equation (15) is subjected to the Laplace transformation at zero initial conditions, an operator equation (16) with transmittance (17) is obtained:

$$\widetilde{\alpha}(s) = G(s)\widetilde{M}_w(s) \tag{16}$$

$$G(s) = \frac{G_0}{\left(\frac{s}{\omega_0}\right)^2 + 2\xi\frac{s}{\omega_0} + 1} \tag{17}$$

The following parameters depending on system parameters can be discerned in the transmittance formula:

$G_0 = \frac{1}{k}$ – system gain factor (18)

$\omega_0 = \sqrt{\frac{k}{J}}$ – characteristic frequency of the breakpoint in the spectral-response curve (19)

$\xi = 0.5\frac{\mu}{\sqrt{Jk}}$ – system damping coefficient (when $\xi \geq 1$, the system does not oscillate) (20)

They make it possible to determine the dynamic properties of the system and facilitate the scaling of the equations.

4. Research software for the simulation and analyses of torsional vibrations in the motorcycle steering system

The research software has been prepared for the Matlab-Simulink (M-S) environment. It makes it possible to simulate nonlinear vibrations in the steering system model, to visualize the computation results with using the phase plane as well, and to carry out extensive numerical research on variously defined sensitivity problems concerning model parameters and input (excitation) signals. This software has been expanded from the one presented in the previous paper [18], which was dedicated to numerical problems related to the simulation of vibrations in the steering system (controlling of the stick-slip process in the neighbourhood of zero velocity and selection of equation integration algorithms and equation parameters).

The first part of the research software is an M-file prepared in the Matlab language and the second one is a simulation model defined in the form of block diagrams implemented in the Simulink environment. The M-file organizes the simulation calculations and their visualization; moreover, the variables and parameters are also defined in it. The model as a whole may be downloaded from the Internet [8].

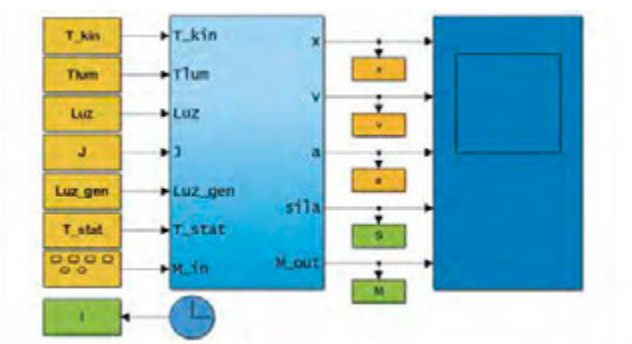

Fig. 7. Schematic diagram of the basic model structure

The schematic diagram in Fig. 8 shows the general block structure of the simulation model. The macro-block includes a detailed schematic diagram of the simulation model (Fig. 9).

The other blocks represent virtual oscilloscope unit to monitor current traces of the quantities observed, clock unit, generator block, and blocks of the "To-Workspace" type, making it possible to export the computation results and to visualize them in the phase plane; the visualization is done from the M file level.

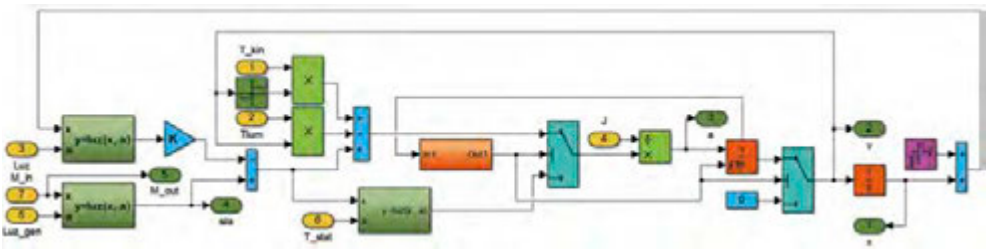

Fig. 8. Simulation model with a "hard zeroing mechanism"

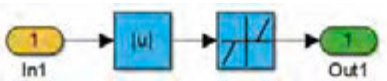

Fig. 9. Singular state detector model

The schematic diagrams shown in Figs. 8 and 9 depict the essence of functioning of the computational model. The system includes singular state detector block, model structure switching block controlled by it, and integrator block calculating the velocity values as a function of time and provided with an additional resetting input and velocity state output. For the whole reset signal duration time, the integrator remains in its initial state. The reset signal is generated by the detector block in a closed loop system, based on the velocity state output signal. This signal becomes available earlier than the standard signal at the integrator output, thanks to which an algebraic loop in the computation process is avoided. The control condition $(\dot{\alpha}(t) \neq 0 \;/\; \dot{\alpha}(t) = 0 \text{ or } |\dot{\alpha}(t)| > \varepsilon$ and $|\dot{\alpha}(t)| \leq \varepsilon)$ is defined in the detector as shown in Fig. 9.

5. Example results of simulation tests and vibration analyses

In consideration of editorial limitations, the simulation tests and vibration analyses discussed here were exclusively oriented at highlighting the advantages of the computation methods presented. Therefore, the attention was chiefly focused on testing the impact of individual parameters of the non-linear $luz(...)$ and $tar(...)$ representations on the vibration modes and their displays in the phase plane at the assumed input (excitation) signal $M_w(t) = M_{w0}sin(\omega t)$. In consideration of a possibility of measurement disturbances, the adding of generated white noise $q(t) = q_0 gen(t)$ to the simulated signals $\alpha(t)$ (Fig. 10) was allowed.

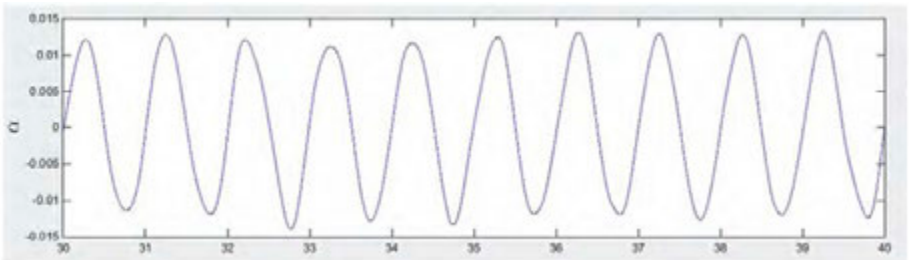

Fig. 10. Time history of the simulated signal *α(t)* with a measurement noise signal imposed onto it

In the tests presented here, the assumed tests values of the model parameters were by no means the data of a real steering system; instead, they were parameters of a scaled model, previously used at the testing of numerical procedures [18]. Below is an example data set used (in the SI system).

Table 1. List of parameters of the simulation model

Notation used	Value	Description
Alfa	0	Initial angle of torsion of the torsional pendulum
Ampl	1	Amplitude of the input signal
Omega	1	Angular frequency of the input signal
K	100	Moment of dry kinetic friction forces
T_stat	0.2	Maximum moment of static friction forces
T_kin	0.2	Moment of dry kinetic friction forces
J	0.5	Moment of inertia
Tlum	0.5	Damping coefficient (for viscous friction)
Luz	0.01	Angular freeplay parameter
Luz_gen	0	Freeplay parameter of the external input generator
e	0.0001	"Hard zeroing" parameter
np	$5 \cdot 10^{-10}$	Amplitude parameter of the measurement noise

Let us note that at the mechanical parameter values such as given above, the transmittance parameters are: G_0 = 0.01, ω_0 = 200, and ξ = 0.03 << 1 and this means that when the excitation exclusively comes from non-zero initial conditions, the response is vibration decaying at quite a low rate, and if an external excitation is the only input applied to the system then vibration with an amplitude reduced to one hundredth may be expected as the response.

Selected results of simulation calculations have been presented below as an example. The computations were carried out for four data sets (variants) for the model of the system under analysis:

- Variant 1 (linear model, with neither freeplay nor dry friction): Luz_0 = 0, T_kin = 0, T_stat = 0;
- Variant 2 (non-linear model, with freeplay but without dry friction): T_kin = 0, T_stat = 0;
- Variant 3 (non-linear model, without freeplay but with dry friction): Luz_0 = 0;
- Variant 4 (non-linear model, with freeplay and dry friction).

To highlight the impact of measurement disturbances (which is a matter of particular interest as regards the Lissajous figures and Poincaré maps), the tests on forced vibrations were carried out with both the absence and presence of measurement disturbances being assumed.

Free vibration tests in the absence of measurement disturbances

In this case, $M_w(t) = 0$ and the system vibration is a result of a non-zero torsion angle at the initial instant (with all the other initial conditions being zero).

The calculation results (Fig. 11) show a considerable impact of freeplay and dry friction on the time curves and phase portraits. In particular, the stick-slip effect is very conspicuous for variant 4, when freeplay and dry friction occur at the same time.

Forced vibration tests in the absence of measurement disturbances

All the initial conditions are zero and the system vibration is a result of a signal $M_w(t) = M_{w0}sin(\omega t)$ applied as an input.

Selected calculation results (Fig. 12) show a considerable impact of freeplay and dry friction on the time curves and on the Lissajous figures and Poincaré maps (α was recorded for $t > 2$ s). Singular non-linear effects can be observed for variants 2, 3, and 4; for variant 4, when freeplay and dry friction occur at the same time.

Forced vibration tests in the presence of measurement disturbances

The test conditions were as specified above, except for the fact that the displays in the phase plane were generated for the $\alpha(t)$ curves being disturbed by measurement noise.

Selected calculation results (Figs. 12 and 13) show a considerable impact of freeplay and dry friction on the time curves and on the Lissajous figures and Poincaré maps. The impact of disturbances was extremely strong for variant 4.

Variant 1 (linear model, with neither freeplay nor dry friction)

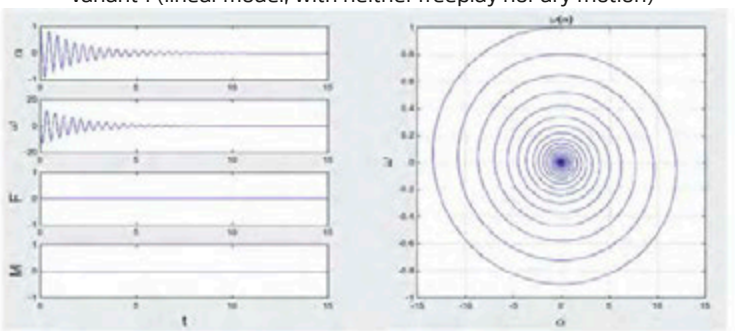

Variant 2 (non-linear model, with freeplay but without dry friction)

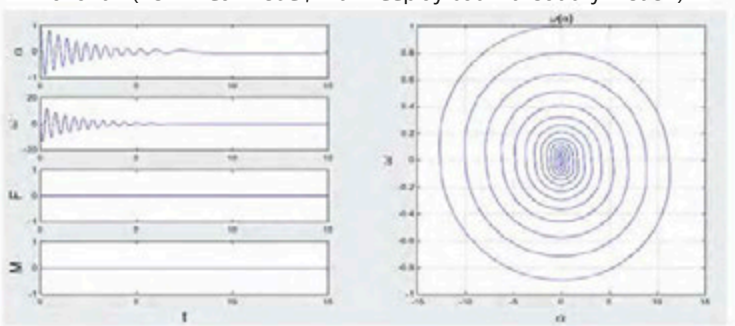

Variant 3 (non-linear model, without freeplay but with dry friction)

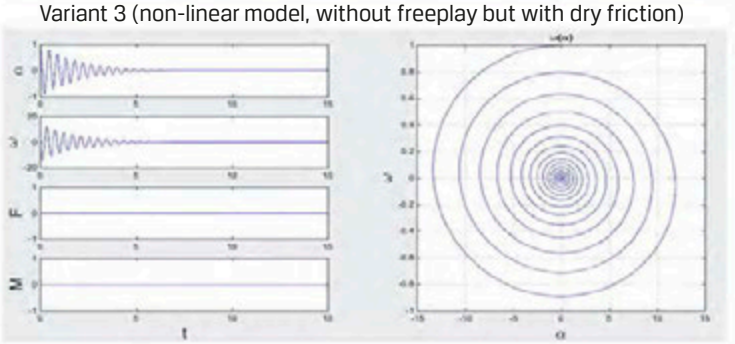

Variant 4 (non-linear model, with freeplay and dry friction)

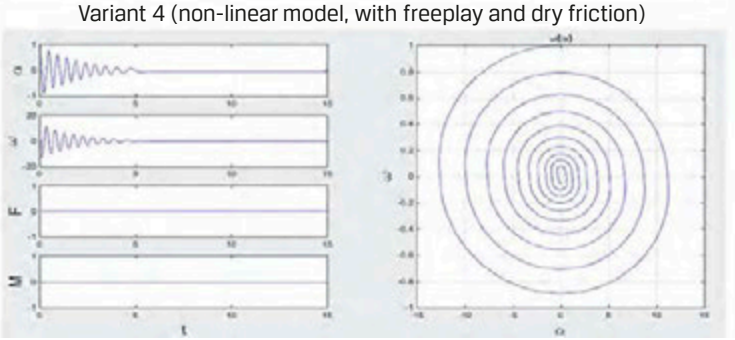

Fig. 11. Results of testing free vibration in the absence of measurement disturbances

Variant 1 (linear model, with neither freeplay nor dry friction)

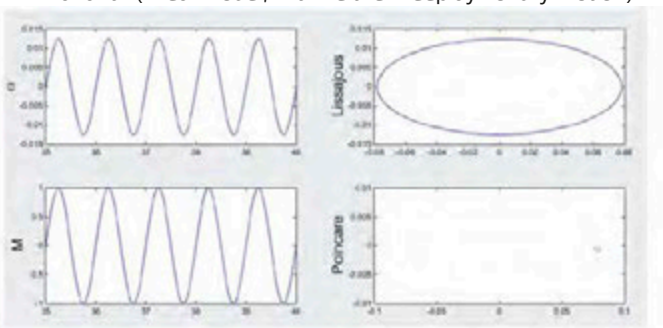

Variant 2 (non-linear model, with freeplay but without dry friction)

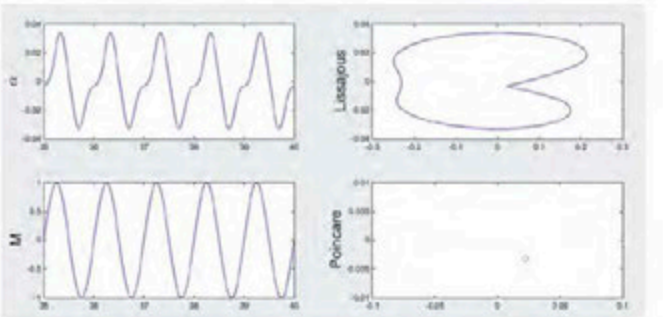

Variant 3 (non-linear model, without freeplay but with dry friction)

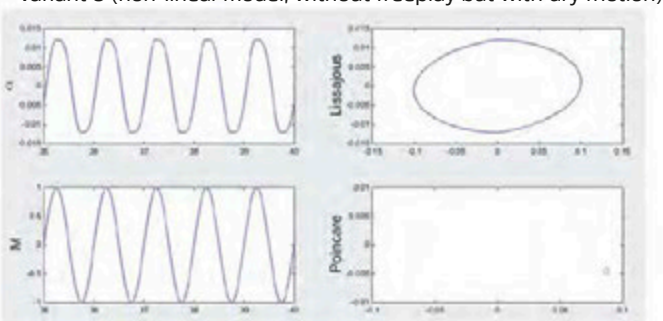

Variant 4 (non-linear model, with freeplay and dry friction)

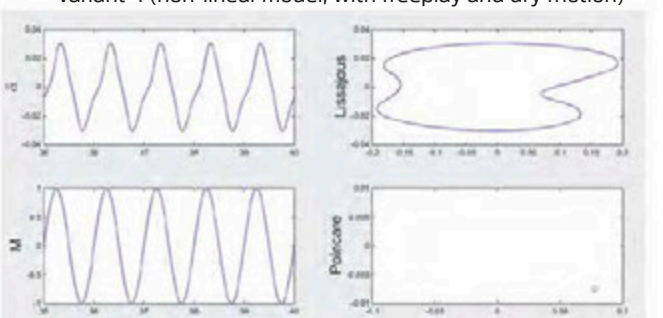

Fig. 12. Results of testing forced vibration in the absence of measurement disturbances

Variant 1 (linear model, with neither freeplay nor dry friction)

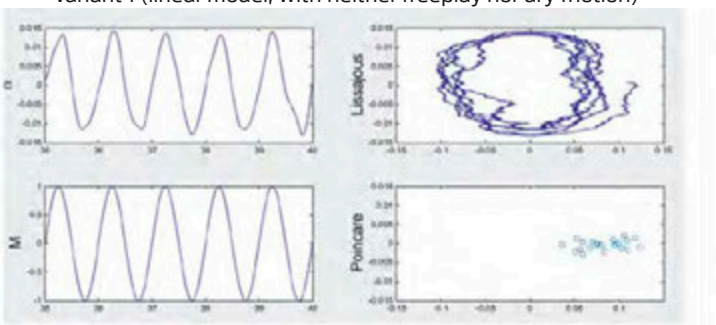

Variant 2 (non-linear model, with freeplay but without dry friction)

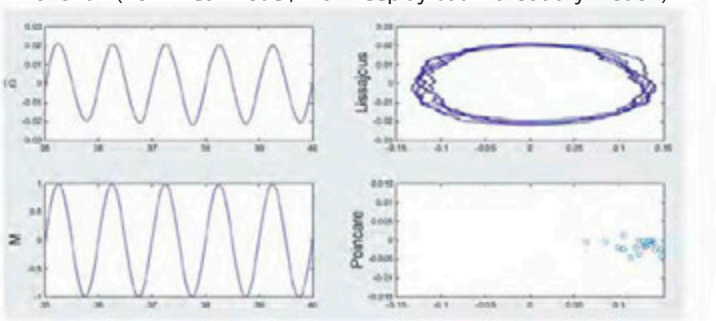

Variant 3 (non-linear model, without freeplay but with dry friction)

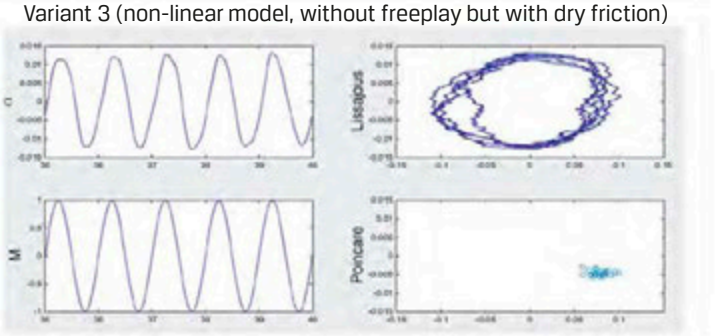

Variant 4 (non-linear model, with freeplay and dry friction)

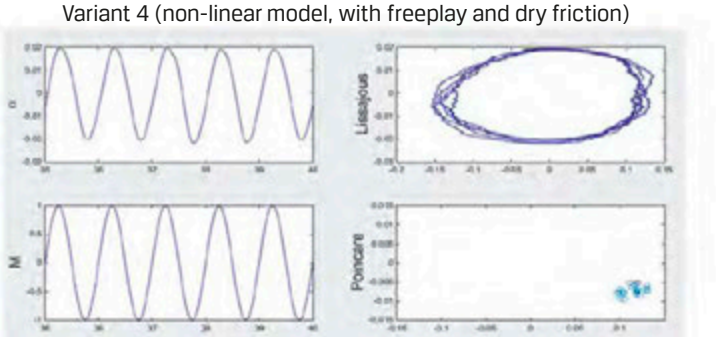

Fig. 13. Results of testing forced vibration in the presence of measurement disturbances

6. Recapitulation

This article presents a method of analysing torsional vibrations in the motorcycle steering system in the phase plane with using the Lissajous figures and Poincaré maps as research tools. For the purposes of presentation of this method and assessment of its capabilities, simulation tests were carried out, where a special test model was used, corresponding to the structure of the steering system model that enabled the simulation of vibrations, including non-linear vibrations generated in the presence of freeplay and friction. The simulation program incorporated a random noise generator, thanks to which the signal curves could be disturbed in a way similar to what takes place in the vibration tests carried out on real objects. The computer simulations made it possible to investigate the impact of changes in the test model parameters on changes in the display forms.

Based on the computational experiments carried out, some fragments of which have been presented herein, a statement may be made that the Lissajous figures and Poincaré maps provide a god tool not only to analyse vibrations but also to identify the vibration reasons. The presence of freeplay and/or friction significantly deforms the ellipse that is obtained as a Lissajous figure in the case of linear vibrations. The appearance of measurement noise can be seen in the Lissajous figures but it is especially identifiable (thanks to the possibility of estimating the harmonic frequencies) by using Poincaré maps.

The use of this method in the analysis of torsional vibrations in the motorcycle steering systems requires multiple simulations to be carried out on a model having a more complicated structure, which should correspond to that of real objects.

The full text of the article is available in Polish online on the website http://archiwummotoryzacji.pl.

Tekst artykułu w polskiej wersji językowej dostępny jest na stronie http://archiwummotoryzacji.pl.

References

[1] Al-Khazali H A H, Askari M R. Geometrical and Graphical Representations Analysis of Lissajous Figures in Rotor Dynamic System. IOSR Journal of Engineering.

[2] Armstrong-Helouvry B, Dupont P, Canudas de Wit C. A Survey of Models, Analysis Tools and Compensation Methods for the Control of Machines with Friction. Automatica, Vol. 30, No. 7, 1994, 1083-1138.

[3] Awrejcewicz J. Matematyczne metody mechaniki (Mathematical methods in mechanics). Wydawnictwo Politechniki Łódzkiej (Publishing House of the Lodz University of Technology), Łódź 1995.

[4] Awrejcewicz J, Lamarque C H. Bifurcation and Chaos in Nonsmooth Mechanical Systems. World Scientific, Singapore 2003.

[5] Brown R, Chua L O. Dynamical synthesis of Poincare maps. International Journal of Bifurcation and Chaos, Vol. 3, No. 5, 1993, 1235-1267.

[6] Cossalter V. Motorcycle dynamics. United Kingdom, 2006.

[7] de Larminat P, Thomas Y. Automatyka – układy liniowe (Automatics – Linear systems). Vol. 1, Sygnały i układy (Signals and systems). WNT Warszawa 1983 (Polish translation).

[8] http://andrzejdebowski.wat.edu.pl/Publikacje.html#about6

[9] Łuczko J. Drgania regularne i chaotyczne w nieliniowych układach mechanicznych (Regular and chaotic vibrations in non-linear mechanical systems). Wydawnictwo Politechniki Krakowskiej (Publishing House of the Cracow University of Technology), Kraków 2008.

[10] Maor E. Trigonometric Delights. Princeton University Press, Princeton 1998.

[11] Osiński Z. (ed.) et al. Tłumienie drgań (Vibration damping). PWN Warszawa 1997.

[12] Pacejka H B. Tyre and vehicle dynamics. Elsevier, Oxford 2012.

[13] Rana A, Mittal H. A Labview Based Simulation of Lissajous Pattern Using DAQ Card. Int. J. of Electronic and Electrical Eng., Vol. 7, No. 2, 2014, pp. 149-158.

[14] Świsulski D. Komputerowa technika pomiarowa: oprogramowanie wirtualnych przyrządów pomiarowych w LabVIEW (Computer measuring technology: LabVIEW-based software for virtual measuring instruments). Agenda Wydawnicza PAK, Warszawa 2005

[15] Żardecki D. Piecewise Linear luz(...) and tar(...) Projections. Part 1 – Theoretical Background. Journal of Theoretical and Applied Mechanics, Vol. 44, No. 1, 2006, pp. 163-184.

[16] Żardecki D. Piecewise Linear luz(...) and tar(...) Projections. Part 2 – Application in Modeling of Dynamic Systems with Freeplay and Friction. Journal of Theoretical and Applied Mechanics, Vol. 44, No. 1, 2006, pp. 185-202.

[17] Żardecki D. Modelowanie luzu i tarcia oparte na odwzorowaniach luz(...) i tar(...) – podstawy teoretyczne i zastosowanie w symulacji drgań nieliniowych w układach kierowniczych samochodów (Freeplay and friction modelling based on the luz(...) and tar(...) representations – theoretical grounds and application in the simulation of nonlinear vibrations in motor vehicle steering systems). Postdoctoral dissertation, Wydawnictwo WAT (Publishing House of the Military University of Technology), Warszawa 2007.

[18] Żardecki D, Dębowski A. Examination of computational procedures from the point of view of their applications in the simulation of torsional vibration in the motorcycle steering system, with freeplay and friction being taken into account. The Archives of Automotive Engineering - Archiwum Motoryzacji. 2014; 64(2): 179-195.